Supplementary Materials

A Decoupled Finite Element Analysis Method for Calculating the Piezoelectric and Flexoelectric Effects in Nanowires

Zhiqiang Zhang[1,2,†], Dalong Geng[2,†], Xudong Wang[2,*]

1.School of Power and Mechanical Engineering, Wuhan University, Wuhan, China

2. Department of Materials Science and Engineering, University of Wisconsin-Madison, Madison, WI 53706, USA

† These authors contributed equally

*Email: xudong.wang@wisc.edu

S1: Fully coupled finite element analysis (FEA) method

Fully coupled FEA method has been used to calculate the piezoelectric effects in most commercial software [1,2]. For each node (i) in an element four degrees of freedom are defined, including three displacements (u_{ix}, u_{iy}, u_{iz}) and one electric potential ($\emptyset_i$).

According to the variation principle and virtual work principle, the static governing equation for piezoelectric materials can be written as

$$\int_V [\{\delta\varepsilon\}^T[c^E]\{\varepsilon\} - \{\delta\varepsilon\}^T[e]^T\{E\} - \{\delta E\}^T[e]\{\varepsilon\} - \{\delta E\}^T[\chi]\{E\} - \{\delta u\}^T\{P_b\} + \delta\emptyset\overline{\sigma}]\, dV - \int_{S_1} \{\delta u\}^T\{\overline{T}\}\, dS + \int_{S_2} \delta\emptyset\overline{\sigma}'\, dS - \{\delta u\}\{P\} + \delta\emptyset Q = 0 \quad \text{(S1)}$$

where $\{P_b\}$, $\{\overline{T}\}$ and $\{P\}$ are body force, surface traction and point force respectively; and $\overline{\sigma}$, $\overline{\sigma}'$ and Q are body charge, surface charge, point charge respectively.

With the help of the shape functions $[N_u]$ and $[N_\emptyset]$ in an element, the displacement field $\{u\}$ and the electric potential $\emptyset$ can be obtained based on the displacement values $\{u_i\}$ and the electric potential $\{\emptyset_i\}$ at each node by following equations.

$$\{u\} = [N_u]\{u_i\} \quad \text{(S2)}$$

$$\emptyset = [N_\emptyset]\{\emptyset_i\} \quad \text{(S3)}$$

After differentiation of equation (S2) and (S3), we can acquire the strain field $\{\varepsilon\}$ and the electric field $\{E\}$.

$$\{\varepsilon\} = [B_u]\{u_i\} \quad \text{(S4)}$$

$$\{E\} = -[B_\emptyset]\{\emptyset_i\} \quad \text{(S5)}$$

where $[B_u]$ and $[B_\emptyset]$ are the shape functions derivatives.

Substitute equations (S2), (S3), (S4) and (S5) into (S1) and the classic fully coupled FEA equations for piezoelectric effect is reached as

$$[K_{uu}]\{u_i\} + [K_{u\emptyset}]\{\emptyset_i\} = \{F_B\} + \{F_S\} + \{F_P\} \quad \text{(S6)}$$

$$[K_{\emptyset u}]\{u_i\} + [K_{\emptyset\emptyset}]\{\emptyset_i\} = \{Q_B\} + \{Q_S\} + \{Q_P\} \quad \text{(S7)}$$

where the terms are defined as below

$$[K_{uu}] = \int_V [B_u]^T [c][B_u]\, dV$$

$$[K_{u\emptyset}] = \int_V [B_u]^T [e][B_\emptyset]\, dV$$

$$[K_{\emptyset u}] = \int_V [B_\emptyset]^T [e][B_u]\, dV$$

$$[K_{\emptyset\emptyset}] = -\int_V [B_\emptyset]^T [\varepsilon][B_\emptyset]\, dV$$

Here $[K_{uu}]$ and $[K_{\emptyset\emptyset}]$ are stiffness matrix and dielectric matrix respectively; $[K_{u\emptyset}]$ and $[K_{\emptyset u}]$ are piezoelectric matrices. $\{F_B\}, \{F_S\}$ and $\{F_P\}$ are body force vector, surface force vector and concentrated force vector respectively; $\{Q_B\}, \{Q_S\}$ and $\{Q_P\}$ are body charge vector, surface charge vector and point charge vector respectively.

Through equation (S6) and (S7) we can calculate the displacement field and electric field respectively. The interaction between these two fields are considered simultaneously by means of the coupled matrices $[K_{u\emptyset}]$ and $[K_{\emptyset u}]$. As a result, the piezoelectric effects can be calculated straightforwardly.

S2: The linear piezoelectric coefficient matrix, the complete expansion of the strain gradient and the direct flexoelectric coefficient matrix:

As discussed in other papers, ZnO and BTO can be approximated as isotropic materials[3,4]. In order to simplify the calculations and compare with results from other references, ZnO and BTO are assumed to be isotropic materials in this paper. The linear piezoelectric coefficient matrix *e* (in the form of 3×6), the complete expansion of the strain gradient $\varepsilon_{jk,l}$ (in the form of 18×1) and the direct flexoelectric coefficient matrix (in the form of 3×18) for ZnO and BTO can be written as [5,6]

$$e_{ijk} = \begin{pmatrix} 0 & 0 & 0 & 0 & e_{15} & 0 \\ 0 & 0 & 0 & e_{15} & 0 & 0 \\ e_{31} & e_{31} & e_{33} & 0 & 0 & 0 \end{pmatrix} \quad \text{(S8)}$$

$$\varepsilon_{jk,l} = [\ \varepsilon_{111} \quad \varepsilon_{112} \quad \varepsilon_{113} \quad \varepsilon_{221} \quad \varepsilon_{222} \quad \varepsilon_{223} \quad \varepsilon_{331} \quad \varepsilon_{332} \quad \varepsilon_{333}$$
$$2\varepsilon_{231} \quad 2\varepsilon_{232} \quad 2\varepsilon_{233} \quad 2\varepsilon_{131} \quad 2\varepsilon_{132} \quad 2\varepsilon_{133} \quad 2\varepsilon_{121} \quad 2\varepsilon_{122} \quad 2\varepsilon_{123}\ ] \quad \text{(S9)}$$

$$\mu_{ijkl} = \begin{bmatrix} \mu_{11} & 0 & 0 & \mu_{14} & 0 & 0 & \mu_{14} & 0 & 0 & 0 & 0 & 0 & 0 & \mu_{111} & 0 & \mu_{111} & 0 \\ 0 & \mu_{14} & 0 & 0 & \mu_{11} & 0 & 0 & \mu_{14} & 0 & 0 & 0 & \mu_{111} & 0 & 0 & 0 & \mu_{111} & 0 & 0 \\ 0 & 0 & \mu_{14} & 0 & 0 & \mu_{14} & 0 & 0 & \mu_{11} & 0 & \mu_{111} & 0 & \mu_{111} & 0 & 0 & 0 & 0 & 0 \end{bmatrix} \quad (S10)$$

S3: Material property constants that were used in the potential calculation

	Elastic constants		Relative dielectric constants		Piezoelectric constants			Flexoelectric constants[1]
	Young's modulus E (GPa)	Poisson ratio ν	$k_{\perp}^{r}$	$k_{\parallel}^{r}$	e_{31} (C/m^2)	e_{33} (C/m^2)	e_{15} (C/m^2)	μ_e nC/m
ZnO	129.0	0.349	7.77	8.91	-0.51	1.22	-0.45	-1
$BaTiO_3$	191.0	0.33	2920	168	-2.69	3.65	21.3	-1

1. Both equivalent flexoelectric constants for ZnO and $BaTiO_3$ are assumed to be -1nC/m.

S4: Calculated nonlinear piezoelectric potential distribution along a ZnO NW

The piezoelectric polarization P_i as a function of mechanical strain ε_j (in Voigt notation) can be written up to the second order in strain as[7]

$$P_i = \sum_{j=1}^{6} e_{ij}\varepsilon_j + \frac{1}{2}\sum_{j,k=1}^{6} B_{ijk}\varepsilon_j\varepsilon_k \quad \text{(S11)}$$

Where e_{ij} is the proper piezoelectric tensor of the unstrained material and B_{ijk} represents the first order change of the piezoelectric tensor with strain, that is, the second order or nonlinear piezoelectric coefficients. The following table is the detailed second order piezoelectric coefficients B_{ijk} for the wurtzite point group material provided by Reference 7. There are eight independent coefficients *a*-*h*. The symbol · indicates vanishing coefficients. The rows (columns) corresponds to the index *i* (*jk*) in B_{ijk}.

11	22	33	44	55	66	12	13	23	45	36	26	16	25	15	35	46	14	24	34	56

1	·	·	·	·	·	·	·	·	·	·	·	·	·	2*b*	2*a*	*c*	*a-b*	·	·	·	·	
2	·	·	·	·	·	·	·	·	·	·	·	·	·	·	·	·	·	2*b*	2*a*	*c*	*a-b*	
3	2*d*	2*d*	*g*	*h*	*h*	*d-e*	2*e*	*f*	*f*	·	·	·	·	·	·	·	·	·	·	·	·	

The eight independent coefficients *a-h* (C/m^2) of ZnO are given as followed showing that the second order coefficients are typically one order of magnitude larger than the linear ones.

2*a*	2*b*	*c*	2*d*	2*e*	*f*	*g*	*h*	e_{15}	e_{31}	e_{33}
3.0	2.5	1.4	3.5	3.7	0	-14.1	0.9	-0.53	-0.68	1.31

Using equation (S11), the three components of the electric polarization P_i are calculated by $P_1 = -0.53\varepsilon_5 - 0.52\varepsilon_3\varepsilon_5$, $P_2 = -0.53\varepsilon_4 - 0.52\varepsilon_3\varepsilon_4$, $P_3 = 1.78\varepsilon_3 - 6.174\varepsilon_3^2 + 0.45\varepsilon_4^2 + 0.45\varepsilon_5^2$. In each equation, the first term is the linear component of the piezoelectric effect, and the rest term(s) are the nonlinear component of the piezoelectric effect (second order contributions). According to the polarization equations above, apparently the nonlinear part of the piezoelectric effect will make more influence with the increase of the strain, especially the direct strain ε_3.

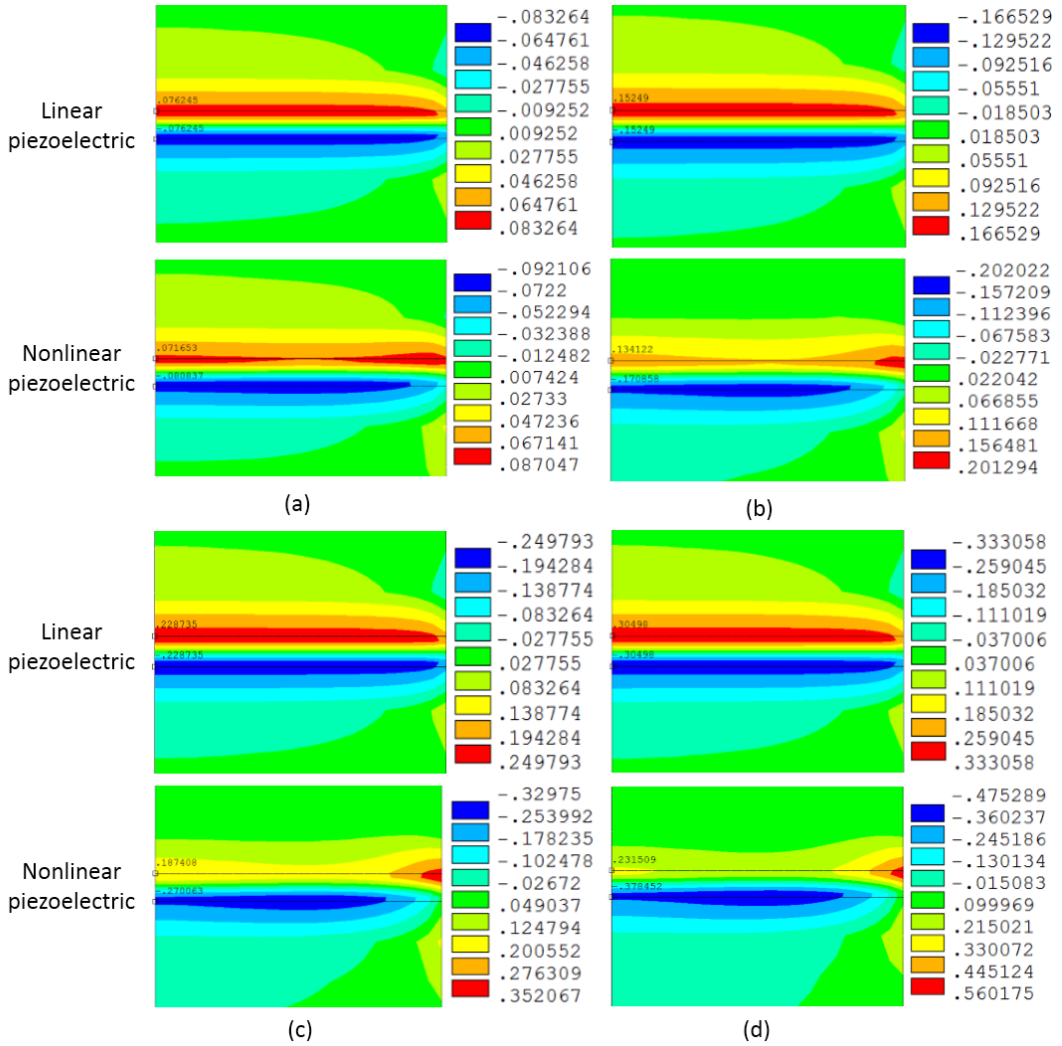

Figure S1. Calculated linear and nonlinear piezoelectric potential distributions along a ZnO NW in cantilever bending mode under four load conditions, $f_y = 20\text{nN}$ (a), $f_y = 40\text{nN}$ (b), $f_y = 60\text{nN}$ (c), and $f_y = 80\text{nN}$ (d).

Using the decoupled FEA method of the article, first we calculated the body charge density and surface charge density of the ZnO NW in cantilever mode, and then applied them on the NW finite element model as boundary conditions. To illustrate and validate the relation between the nonlinear piezoelectric effect and the strain, we adjusted the quantity of the load, and calculated four conditions: $f_y = 20\text{nN}$, 40nN, 60nN and 80nN, respectively. The potential distribution results of the cantilever mode are shown in the Figure S1.

The figure gives the linear and nonlinear piezoelectric potential distributions along the axial cross section under four load conditions, and also gives the potential values of top and bottom nodes of the free end. From the results, with the increase of the load, the nonlinear piezoelectric effect becomes stronger. The potential maximum in the tension region of the NW moves to the fixed end, and conversely the potential minimum in the compression region moves to the free end when the load increases. In all the four load conditions, the maximum absolute value of

potential are all increased, and when $f_y = 80$nN the increment exceeds 50%, but the changes of potential values of top and bottom nodes of the free end are small because there is little direct strain ($\varepsilon_1 = \varepsilon_2 = \varepsilon_3 = 0$) at this end surface.

The linear and nonlinear piezoelectric potential distribution results of the three-point and four-point bending modes are shown in the Figure S2. From the results, because the direct strain is less than that of the cantilever mode under the same load $f_y = 80$nN, less nonlinear piezoelectric effect is induced compared to the cantilever mode. Similarly, to the case of linear piezoelectric effect, there is no potential at the middle segment under three-point and four-point bending modes.

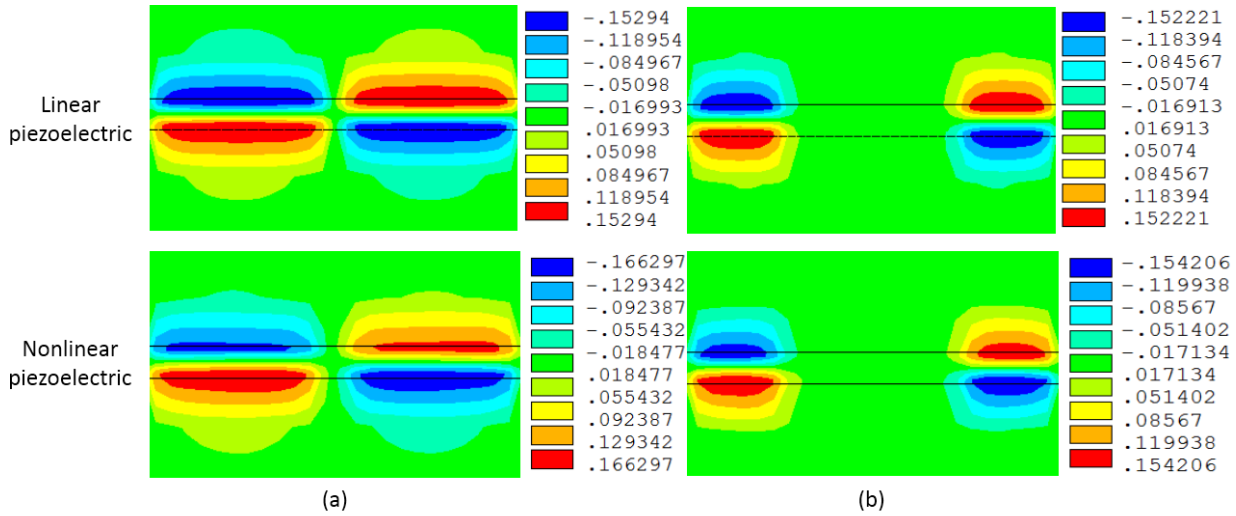

Figure S2. Calculated linear and nonlinear piezoelectric potential distributions along a ZnO NW in the two bending modes. (a) 3-point bending mode, $f_y = 80$nN is applied at the middle of the NW. (b) 4-point bending mode, $f_y = 40$nN is separately applied at two points of the NW middle segment.

S5: Calculated piezoelectric and flexoelectric potential distribution along a ZnO NW

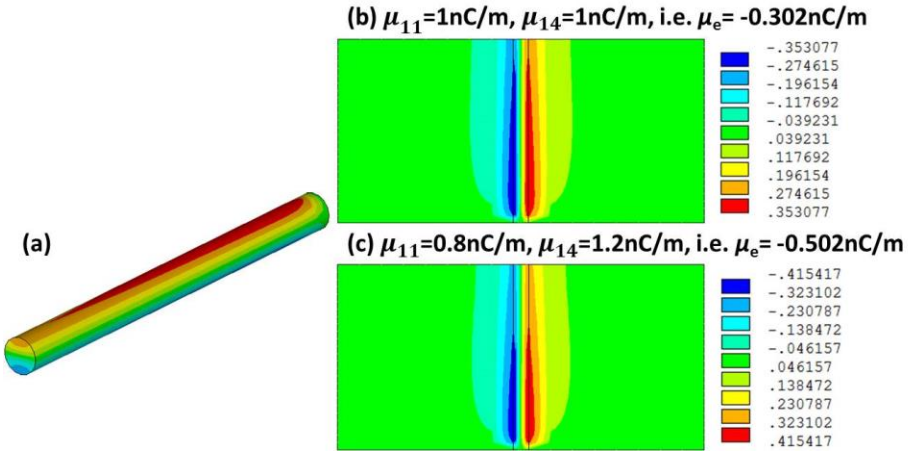

Figure S3. Calculated piezoelectric and flexoelectric potential distribution along a ZnO NW in cantilever bending mode. **(a)** 3D piezoelectric and flexoelectric potential distributions along a ZnO NW beam. **(b)** The potential distributions along the length direction when μ_e= -0.302nC/m. **(c)** The potential distributions along the length direction when μ_e= -0.502nC/m.

S6: Calculated piezoelectric potential distribution along a BTO NW using two methods

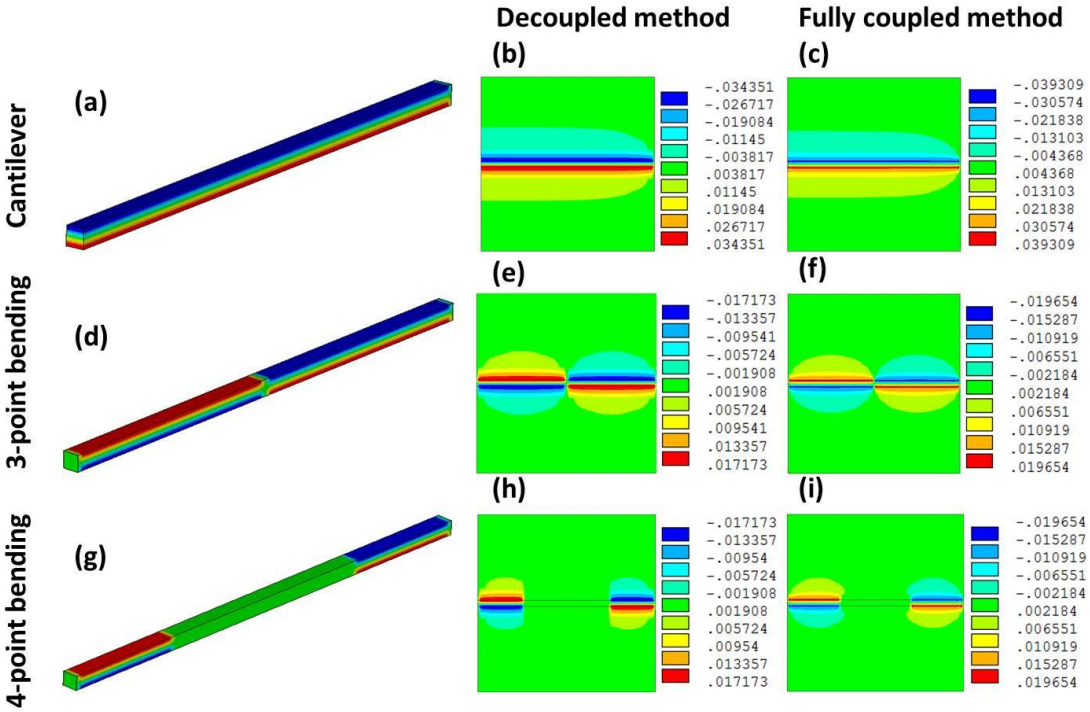

Figure S4. Calculated piezoelectric potential distribution along a BTO using two methods. Study case of a cantilever bending mode **(a-c)**, 3-point bending mode **(d-f)**, and 4-point bending mode **(g-i)**. **(a, d, g)** 3D piezoelectric potential distributions along a ZnO NW beam calculated by

decoupled method. **(b, e, h)** The potential distributions along the length direction calculated by decoupled method. **(c, f, i)** The potential distributions along the length direction calculated by fully coupled method.

Reference:

[1] H. Allik and T. J. R. Hughes, International Journal for Numerical Methods in Engineering **2,** 7 (1970).

[2] A. Kumar, A. Sharma, R. Kumar, R. Vaish, and V. S. Chauhan, Journal of Asian Ceramic Societies **2,** 138 (2014).

[3] C. Liu, S. Hu, and S. Shen, Smart Materials & Structures **21,** 115024 (2012).

[4] C. L. Sun, J. A. Shi, and X. D. Wang, Journal of Applied Physics **108,** 034309 (2010).

[5] H. L. Quang and Q. C. He, Proceedings of the Royal Society A **467,** 2369 (2011).

[6] L. Shu, X. Wei, T. Pang, X. Yao, and C. Wang, Journal of Applied Physics **110,** 104106 (2011).

[7] P.-Y. Prodhomme, A. Beya-Wakata, and G. Bester, Physical Review B **88** (2013).